ISSN: 1410-8917
Jurnal Kimia Sains & Aplikasi
e-ISSN: 2597-9914

Jurnal Kimia Sains dan Aplikasi 26 (8) (2023): 318-323

Jurnal Kimia Sains dan Aplikasi
Journal of Scientific and Applied Chemistry

Journal homepage: http://ejournal.undip.ac.id/index.php/ksa

In Silico DFT (Density Functional Theory) Study of Chemosensor Selectivity of 3-Oxo-3*H*-Benzo[*f*]chromen-2-Carboxylic Acid (ABKK) on Sodium Metal Ion Using FMO (Frontier Molecular Orbital) Analysis

Jamaludin Al-Anshori [1,*], Ajar Faflul Abror [1], Juliandri [1], Agus Safari [1], Ace T. Hidayat [1]

[1]Department of Chemistry, Faculty of Mathematics and Natural Sciences, Universitas Padjadjaran, Sumedang, Indonesia

* Corresponding author: jamaludin.al.anshori@unpad.ac.id

https://doi.org/10.14710/jksa.26.8.318-323

Article Info

Article history:

Received: 13th October 2023
Revised: 06th November 2023
Accepted: 14th November 2023
Online: 15th November 2023

Keywords:
Chemosensor; sodium ion; DFT; FMO; bandgap

Abstract

The chemosensor selectivity of 3-oxo-3*H*-benzo[*f*]chromen-2-carboxylic acid (ABKK) toward Na^+ metal ion has been successfully studied in silico using FMO (Frontier Molecular Orbital) analysis method. The geometry of the ABKK structure was optimized by the DFT (Density Functional Theory) method with a function/basis set: M06/6-31G (*d, p*). Afterward, the electronic properties of the ABKK structure before and after binding to sodium ion were analyzed and compared with the ABKK+other metal ion structures representing valence charges 1-3 and within the constraints of the basis set used. The results of geometry optimization showed that 1ABKK+Na^+ has a more positive frequency/minima than 2ABKK+Na^+ with interaction energies of 145 and 200.5 kcal/mol, respectively. Ignoring the role of solvents, FMO analysis revealed that the bandgap energy of fluorophore and receptor interactions (ΔE LUMO Fl-Rs 1ABKK+Na^+) and (ΔE HOMO Fl-Rs 2ABKK+Na^+) were 0.631 and 0.336 eV, correspondingly. In addition, the bandgap energy of fluorophore/ΔE Fl 1ABKK+Na^+ and 2ABKK+Na^+ were calculated at 4.347 and 4.362 eV. Comparing those two types of bandgap energies with the bandgap belonging to ABKK+other metal ions, the excitation, and PET (Photoinduced Electron Transfer) processes were estimated to be relatively favorable experienced by 2ABKK+Na^+. Finally, the selectivity of ABKK toward sodium metal ions from the computational calculations was relatively in agreement with the laboratory experimental results.

1. Introduction

Chemosensors are sensor-type chemical compounds that can provide accurate information in real-time about the presence of specific compounds or ions in even complex samples. Metal ion chemosensors based on fluorescent compounds work by chelating metal ions contained in the analyte, thus forming a complex followed by changes in fluorescence intensity that can be monitored by spectrofluorometry [1, 2]. Among several metal analysis techniques, chemosensors have advantages over other methods, including low cost, convenience, and fast response [3, 4, 5, 6]. Fluorescent chemosensors consist of two parts, namely, the fluorophore and the receptor. The fluorophore part functions as a signal marker in the form of fluorescence intensity, while the receptor part functions as the binding site of the analyte, which can be a cation [3, 7, 8], anion, or neutral species [9, 10].

Some studies reported that the interaction of chemosensor compounds and metal ions could be explained using DFT computational methods at a level of function/basis set M06/6-31G (*d, p*) [3], B3LYP/6-311+G(d) [7], and B3LYP/LanL2DZ [11]. Further studies of the electronic distribution of HOMO and LUMO at molecular orbitals of the optimized fluorophores and receptors have been shown to explain the mechanism of interaction. Specifically, through Frontier Orbital Molecule (FMO) analysis [12], which studied the

interaction mechanism of HOMO-LUMO of donor-acceptor of chemosensor bearing coumarin aromatic skeleton [3], aromatic Schiff base [7], aromatic β-naphthol [8], and heteroaromatic BODIPY [11], the probability of whether or not the PET (Photoinduced electron transfer) process occurs can be estimated [13, 14, 15]. Especially for chemosensors with coumarin aromatic structure, Mergu *et al.* [3] have successfully validated the selectivity data and mechanism of its chemosensor interaction against Cu^{2+} ion using DFT computational methods at the M06 level theory with a basis set of 6-31G (*d, p*). Studying the interaction mechanism between a chemosensor receptor and a substrate is critical in developing chemosensor applications in various fields such as medicine, clinics, catalysts, environmental chemistry [13, 14, 15], biology, and foods [16, 17].

One of the organic compounds that can be used as chemosensors is coumarin derivatives, which have advantages such as large Stockes shift, high fluorescent quantum yield, good light stability, absorption and emission profile in visible light regions, and non-toxic [18]. Among the many coumarin-derived compounds that have been successfully reported as selective and sensitive chemosensors to Na^+ metal ion was 3-oxo-3*H*-benzo[*f*]chromen-2-carboxylic acid (ABKK) with an "on- off" chemosensor model through fluorescence quenching by oxidative and reductive PET [2].

To the best of our knowledge, the selectivity of the ABKK interaction towards Na^+ metal ion, among others, has never been studied. Therefore, researchers are interested in further investigating the interaction mechanism of ABKK with Na^+ metal ions compared to other metal ions in silico with an FMO analysis approach. Perhaps the computational study of ABKK selectivity towards Na^+ metal ion obtained can be used to design further the derivative structure of ABKK that can be selective against other metal ions. In the end, ABKK compound and their derivatives can be applied more widely in health, environment, and food. The in silico method is the leading choice in studying the mechanism of chemosensor interaction with the substrate because it is considered more economical than a laboratory experiment.

2. Experimental

2.1. Materials and Tools

The materials used in this study were the ABKK structure model and several representative models of valence metal ions of 1, 2, and 3, including Na^+, K^+, Li^+, Mg^{2+}, Ni^{2+}, Cu^{2+}, and Al^{3+} ions. The type of metal ions was selected based on the laboratory test results [2] and the basis set's limitations. DFT calculation was performed on a PC with Intel®Xeon(R) Processor CPU E5-2650 v2@2.60 GHz ×32, 16 GB RAM, with Gaussian 09 software [19].

2.2. Procedures

2.2.1. Computational Calculations

Computational calculation methods were adapted from the procedure reported by Mergu *et al.* [3] to study the mechanism of interaction of coumarin-skeleton chemosensors and their derivatives with metal ions. The structure of the ABKK chemosensor and its chelate compound with Na^+, K^+, Li^+, Mg^{2+}, Ni^{2+}, Cu^{2+}, and Al^{3+} metal ions was optimized at 1:1 and 2:1 ratios under non- solvent conditions using the DFT at the level of M06 method with a basis set of 6-31G (*d, p*) [3, 19]. The optimization ratio of ABKK to metal ions was based on the results of fluorimetric titration of ABKK with metal ions in the laboratory [2]. Next, the electronic properties of the molecular orbital of ABKK and its chelates with metal ions were analyzed.

The molecular orbitals of HOMO and LUMO (benzocoumarin fluorophores and carboxylate receptors) and their energy differences ($\Delta E_{HOMO-LUMO}$) were investigated at the same theoretical level. The energy data of HOMO-LUMO generated from optimized molecular geometry were further studied in its interaction with the FMO analysis [3, 7, 8, 11]. In addition, the interaction energy of the chemosensor-metal ion [7], basis set superposition error (BSSE) [20], and the vibrational frequency were also calculated. The calculation method was also validated by comparing the measured infra-red spectral frequency with the calculated one.

3. Results and Discussion

3.1. Geometry Optimization and FMO Analysis of ABKK Structure

The method of structural optimization of ABKK with a benzocoumarin framework in this study was adapted from the process of the geometric optimizing structure of coumarin derivative compounds, DFT-M06, basis set 6- 31G(*d, p*) [3], where the DFT M06 method belongs to the functional meta-GGA class with 27% HF exchange and is very well used to calculate non-covalent interactions, thermochemistry of transition metals, organometals [21] and electronic excitation energy [22]. Based on the results of the geometry optimization of the ABKK, a positive vibrational frequency value was obtained (Figure 1). The value indicated that the structure of the ABKK has reached a stable form with a minima state. The optimization results have also been confirmed by the emergence of vibrational absorption of O-H stretching, C=O (carboxylate) stretching, and C=O (lactone) stretching at wavenumbers of 3543, 1892, and 1821 cm^{-1}, respectively. The vibrational absorption of the three main groups of ABKK was in the range of tolerant frequency differences (±100 cm^{-1}) against the FTIR results of ABKK from the laboratory [2].

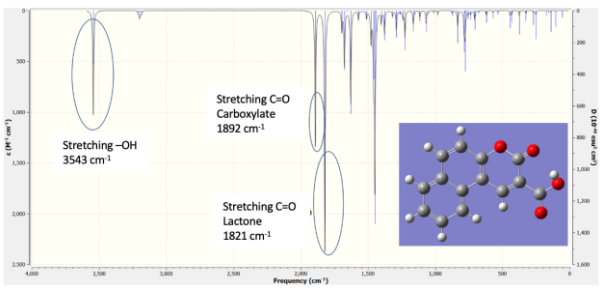

Figure 1. The calculated vibration frequency of ABKK in a minima state

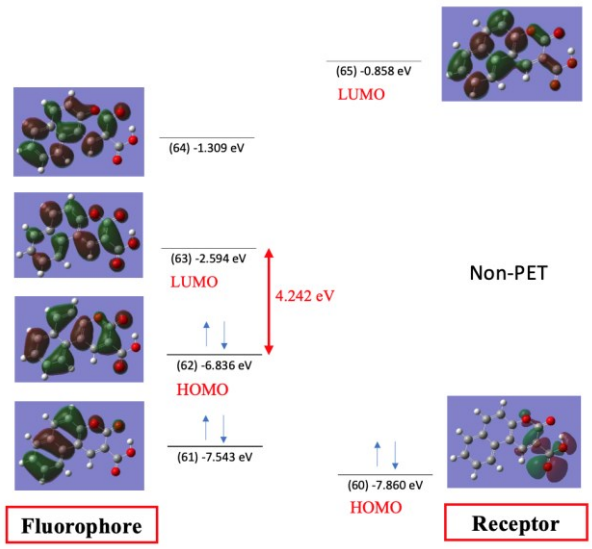

Figure 2. Calculated HOMO-LUMO energy of ABKK, optimized by DFT-M06, basis set 6-31G(*d*, *p*). Molecular orbital of fluorophore (left) and receptor (right)

Furthermore, from the results of optimized ABBK, the HOMO-LUMO energy of molecular orbitals was also obtained (Figure 2). In addition, their electron distribution (green and red clouds) was also achieved, representing part of fluorophore and receptor groups. The moiety of fluorophore, which acts as a fluorescence signaling unit, was represented by a benzocoumarin group. In contrast, the receptor, which acts as a metal ion binding site, was expressed by a carboxylate group. Computational data revealed that the benzocoumarin fluorophore has HOMO and LUMO energies of -6.836 eV and -2.594 eV, respectively. With a bandgap energy of 4.242 eV, thus the benzocoumarin group will be relatively favorable to undergo excitation and decay through the fluorescence process without being quenched by an electron transfer from the carboxylic receptor, which has lower HOMO energy than the HOMO of fluorophore one (ΔE = 1.024 eV) (Figure 2). Thereby, no PET occurred (non-PET).

3.2. Geometry Optimization and FMO Analysis of ABKK+Na^+ Structure

The geometry optimization of one and two equivalents of ABKK compound chelating one equivalent of Na^+ metal ion was carried out by the same method as the optimization of ABKK without metal ion, DFT-M06, basis set 6-31G(*d*, *p*) (Figure 3). The results revealed a positive vibrational frequency of 1ABKK+Na^+ (Figure 4). Moreover, the optimized 1ABKK+Na^+ also exhibited more minima/positive frequency values than 2ABKK+Na^+ with the first three frequency values of 28, 45, and 61 cm^{-1} (1ABKK+Na^+) and 10, 11, and 20 cm^{-1} (2ABKK+Na^+). It was implied that the structure of 1ABKK+Na^+ has reached a stable form with the minima state. The data was also reinforced by the interaction energy of 1ABKK+Na^+ (145 kcal/mol), which was 55.5 kcal/mol lower than the interaction energy of 2ABKK+Na^+ (200.5 kcal/mol) (Figure 3), with the BSSE correction values being -145 and -200.5 kcal/mol, respectively.

Furthermore, the optimization also resulted in bandgap energy of chelating one and two equivalents of ABKK with one equivalent of Na^+, with the values of ΔE Fl of 4.347 and 4.362 eV, respectively (Figure 5). In particular, the compound 1ABKK+Na^+ showed a receptor value of LUMO of -2.199 eV and HOMO of -6.579 eV. In the meanwhile, the energy of HOMO and LUMO of the fluorophores were -5.915 and -1.568 eV, respectively (Figure 5). According to FMO analysis, the low bandgap energy between the LUMO of the receptor and the LUMO of the fluorophore (0.631 eV) allows the transfer of excited fluorophore electrons to the LUMO of the receptor. Afterward, the electrons will be transferred back to the HOMO of the fluorophore, resulting in a fluorescence quenching through the Intermolecular Charge Transfer (ICT) process [3]. This mechanism was recognized as the oxidative PET, which will reduce the fluorescence intensity of the ABKK compound. Similar phenomena are also found in several other models of chemosensor compounds [13, 14, 15].

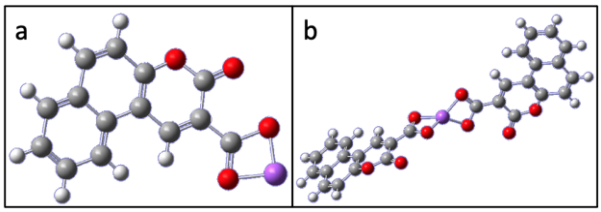

Figure 3. Optimized geometries of (a) 1ABKK+Na^+ ($E_{interaction}$ 145 kcal/mol) and (b) 2ABKK+Na^+ ($E_{interaction}$ 200.5 kcal/mol)

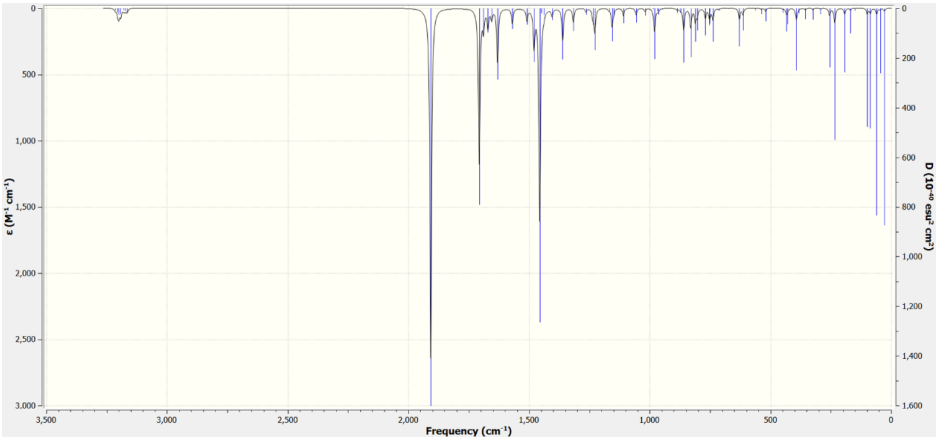

Figure 4. Calculated vibrational frequency of 1ABKK+Na^+ in a minimum state

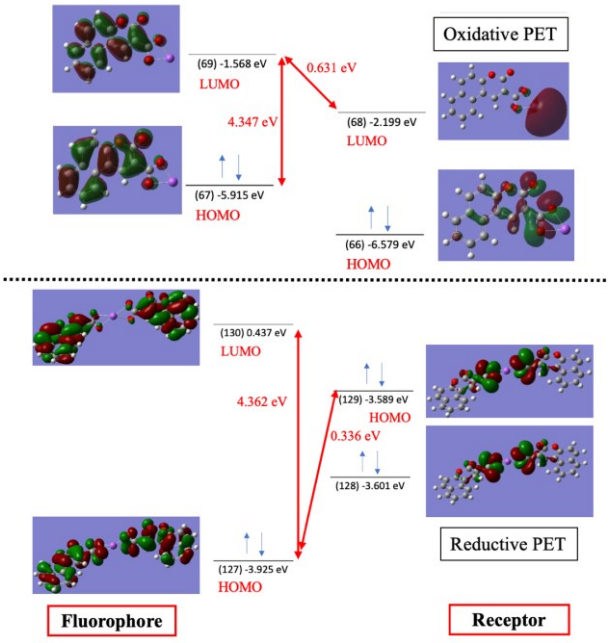

Figure 5. Calculated bandgap energy of HOMO-LUMO fluorophores and receptors and their FMO analysis. 2ABKK+Na^+ (reductive PET), 1ABKK+Na^+ (oxidative PET)

On the other side, 2ABKK+Na^+ gave a HOMO value of the receptor of -3.589 eV and HOMO and LUMO values of the fluorophore of -3.925 and 0.437 eV, respectively (Figure 5). The FMO analysis revealed that the greater value of the HOMO receptor than the HOMO fluorophore allows for the electron transfer from the HOMO of the receptor to the already excited HOMO of the fluorophore. As a result, the HOMO electron of the fluorophore that has been excited to its LUMO cannot return to its origin of HOMO. The mechanism was recognized as reductive PET, which can cause a decrease in the fluorescence intensity of the ABKK compound. Several published chemosensor models with similar mechanisms align with this [13, 14, 15].

3.3. Geometry Optimization and FMO Analysis of ABKK+Other Metal Ions

The geometry optimization of the ABKK structure with several metal ions was carried out by using one and two equivalents of the ligand with one equivalent of another metal ion, including K^+, Li^+, Mg^{2+}, Ni^{2+}, Cu^{2+}, and Al^{3+}, following metal ions tested in the laboratory against ABKK compound [2]. In addition, the typical metal ions selected in this geometry optimization were limited by the basis set 6-31G, which cannot be used to calculate larger atomic orbitals such as *d* and *f* orbitals. For the geometry optimization data of ABKK compounds that interact with various metal ions to be compared equally with each other, the optimization of ABKK geometry with various metal ions also used a similar method as before, namely M06/6-31G(d, *p*) with the total charge considered according to the sum of the charges of ligands and metal ions.

The results of geometry optimization and FMO analysis are presented in Table 1. The data were then used to study the selectivity of ABKK compound against Na^+ instead of other metal ions by considering several factors, including the small bandgap energy value of the fluorophore and PET's short oxidative or reductive distance. The small bandgap energy value of the fluorophore allows chemosensor compounds to excite their electrons by absorbing the required energy that is not too large. The short oxidative and reductive distances of PET allow electron transfer between the fluorophore and receptor to occur more favorably than over long distances so that the PET mechanisms can arise [13, 14, 15].

Table 1. Data of FMO analysis and bandgap energy values of HOMO-LUMO fluorophore (Fl) and receptor (Rs) of ABKK and metal ions

ABKK/eq	Metal Ion (1 eq)	HOMO Fl/eV	LUMO Fl/eV	HOMO Rs/eV	LUMO Rs/eV	ΔE Fl/eV	ΔE LUMO Fl-Rs (Oxd PET)/eV	ΔE HOMO Fl-Rs (Red PET)/eV
1	Na^+	-5.915	-1.568	-6.579	-2.199	4.347	0.631	
1	Li^+	-6.163	-1.870	-7.126	-2.092	4.293	0.222	
1	K^+	-5.724	-1.353	-6.114	-2.208	4.371	0.855	
1	Ni^{2+}	-9.667	-6.245	-11.375	-7.771	3.422	1.526	
1	Cu^{2+}	-9.563	-6.096	-11.269	-7.327	3.467	1.231	
1	Mg^{2+}	-9.117	-3.480	-10.695	-7.529	5.637	4.049	
1	Al^{3+}	-14.589	-7.784	-13.654	-11.911	6.805	4.127	
2	Na^+	-3.925	0.437	-3.589	>1.430	4.362		0.336
2	Li^+	-3.989	0.431	-3.703	>1.737	4.420		0.286
2	K^+	-3.889	0.466	-3.748	-3.482	4.355	3.948	
2	Ni^{2+}	-6.630	-6.513	-6.739	-1.194	0.117		
2	Cu^{2+}	-6.565	-2.454	-7.056	>-1.035	4.111		
2	Mg^{2+}	-6.540	-2.364	-7.785	-0.046	4.176		
2	Al^{3+}	-9.248	-2.937	-10.844	-5.738	6.311	2.801	

Note: Fl=Fluorophore, Rs=Receptor

FMO analysis of 1ABKK+1 metal ion. The optimized geometry of each 1ABKK+Mg^{2+} and +Al^{3+} ions provided a very high bandgap energy value so that the energy required for electron excitation in HOMO will be relatively large. In addition, the considerable distance of the LUMO of the fluorophore to the receptor also inhibited electron transfer. As a result, the quenching process of the ABKK compound by the two metal ions was also tricky, as found in the previous lab testing [2]. On the other hand, although the bandgap energy values of the HOMO-LUMO of 1ABKK+Ni^{2+} and +Cu^{2+} ions were smaller than with the alkali metals (3.4 eV), the bandgap interaction between the LUMO of the fluorophore and the receptor was quite significant when compared to the small values for Na^+, Li^+, and K^+ (<1 eV). The smaller the bandgap interaction, the easier it will be in the oxidative process of PET. For the Li^+ metal ion, the bandgap energy value of the HOMO-LUMO and the distance to the occurrence of oxidative PET obtained were smaller than for the others (4.293 eV). These results did not match the results of lab tests [2], so the ABKK structure with Li^+ metal ion was further optimized using a two-ligand approach.

FMO analysis of 2ABKK+1 metal ion. Upon addition of Ni^{2+}, Cu^{2+}, and Mg^{2+} ions to the two equivalents of ABKK, no oxidative and reductive value of PET was obtained upon a geometry optimization. This was because of no effect of HOMO-LUMO of the receptors on the excitation process of the fluorophores. In this mechanism, the PET and fluorescence quenching did not occur (Non-PET). The results of FMO analysis of two equivalents of ABKK with three alkali metals (+Na^+, +K^+, +Li^+) looked mutually competitive. Although the 2ABKK+K^+ showed a smaller bandgap energy than the Na^+ and Li^+ ions, it has a considerable oxidative PET distance, so it was implied to be less selective to the ABKK compound.

For Na^+ and Li^+ metal ions, the bandgap energy values were calculated at 4.362 and 4.420 eV, respectively, with a difference of 0.058 eV. Meanwhile, the PET's reductive path produced bandgap energies of 0.336 and 0.286 with a difference of 0.05 eV. Based on the bandgap between the two metal ions, 2ABBK+Na^+ will be more favorable to undergo an electronic excitation than toward the Li^+ metal ion so that the unpair electron at the excited HOMO of the fluorophore could be refilled by the electron, transferred from the HOMO of the receptor. Consequently, a fluorescence quenching occurred, as was observed in the laboratory experiment conducted by Al Anshori *et al.* [2].

Overall, the computational calculations are relatively in line with the laboratory results. However, the accuracy of the calculation results must be further improved, including by considering the presence of MeOH: H_2O solvents in the computational process. The presence of MeOH: H_2O solvents was proven to cause redshift of ABKK emission spectra up to ±10 nm when titrated with Na^+ ion [2]. The phenomenon was implied to result from a dipolar interaction between ABKK+Na^+ and the solvents of MeOH: H_2O, resulting in a decrease in excitation energy [23].

4. Conclusion

Based on computational calculations of DFT-M06, a basis set of 6-31G(*d*, *p*), optimized 1ABKK+Na^+ was relatively more stable than 2ABKK+Na^+ due to a more positive/minima frequency and lower interaction energy. FMO analysis revealed that 2ABKK+Na^+ was the most favorable to experience an electronic excitation among other chelated ABKK+ion compounds because of the lowest ΔE Fl value (4.362 eV). In addition, 2ABKK+Na^+ also has a relatively small value of ΔE HOMO Fl-Rs (0.336 eV), making it easier for PET to take place. In general, these results relatively supported ABKK selectivity data on Na^+ ions laboratory tests. However, using solvents in computational calculations is expected to improve calculations' accuracy and suitability with laboratory results.

Acknowledgment

The author would like to thank Universitas Padjadjaran for the support of the RKDU Grant (1549/UN6.3.1/PT.00/2023) and also the ALG Grant of Prof. Ace T. Hidayat (1549/UN6.3.1/PT.00/2023).

References

[1] Sri Wahyuni, Rimadani Pratiwi, Penggunaan Kemosensor Untuk Mendeteksi Ion Logam, *Farmaka*, 4, 3, 1-17

[2] Jamaludin Al Anshori, Andi Rahim, Ajar Faflul Abror, Ika Wiani Hidayat, Tri Mayanti, Muhammad Yusuf, Juliandri Juliandri, Ace Tatang Hidayat, Sodium ion chemosensor of 3-oxo-3*H*-benzo[*f*]chromene-2-carboxylic acid: An experimental and computational study: Scientific paper, *Journal of the Serbian Chemical Society*, 86, 10, (2021), 971-982 https://doi.org/10.2298/JSC200929022A

[3] Naveen Mergu, Myeongjin Kim, Young- A. Son, A coumarin-derived Cu^{2+}-fluorescent chemosensor and its direct application in aqueous media, *Spectrochimica Acta Part A: Molecular and Biomolecular Spectroscopy*, 188, (2018), 571-580 https://doi.org/10.1016/j.saa.2017.07.047

[4] Vinod Kumar Gupta, Naveen Mergu, Lokesh Kumar Kumawat, Ashok Kumar Singh, A reversible fluorescence "off–on–off" sensor for sequential detection of aluminum and acetate/fluoride ions, *Talanta*, 144, (2015), 80-89 https://doi.org/10.1016/j.talanta.2015.05.053

[5] Naveen Mergu, Ashok Kumar Singh, Vinod Kumar Gupta, Highly Sensitive and Selective Colorimetric and Off-On Fluorescent Reversible Chemosensors for Al^{3+} Based on the Rhodamine Fluorophore, *Sensors*, 15, 4, (2015), 9097-9111 https://doi.org/10.3390/s150409097

[6] Vinod Kumar Gupta, Ashok Kumar Singh, Naveen Mergu, Antipyrine based Schiff bases as Turn-on Fluorescent sensors for Al (III) ion, *Electrochimica Acta*, 117, (2014), 405-412 https://doi.org/10.1016/j.electacta.2013.11.143

[7] Ismail Abdulazeez, Chanbasha Basheer, Abdulaziz A. Al-Saadi, A selective detection approach for copper(ii) ions using a hydrazone-based colorimetric sensor: spectroscopic and DFT study, *RSC Advances*, 8, 70, (2018), 39983-39991 https://doi.org/10.1039/C8RA08807A

[8] Jamaludin Al Anshori, Daliah Ismalah, Ajar Faflul Abror, Achmad Zainuddin, Ika Wiani Hidayat, Muhammad Yusuf, Rani Maharani, Ace Tatang Hidayat, A new highly selective "off–on" typical chemosensor of Al^{3+}, 1-((*Z*)-((*E*)-(3,5-dichloro-2-hydroxybenzylidene)hydrazono)methyl) naphthalene-2-ol, an experimental and *in silico* study, *RSC Advances*, 12, 5, (2022), 2972-2979 https://doi.org/10.1039/D1RA08232A

[9] Ruslan Guliyev, Design strategies for chemosensors and their applications in molecular scale logic gates, Bilkent Universitesi (Turkey), 2013

[10] Teresa L. Mako, Joan M. Racicot, Mindy Levine, Supramolecular Luminescent Sensors, *Chemical Reviews*, 119, 1, (2019), 322-477 https://doi.org/10.1021/acs.chemrev.8b00260

[11] Tasawan Keawwangchai, Nongnit Morakot, Banchob Wanno, Fluorescent sensors based on BODIPY derivatives for aluminium ion recognition: an experimental and theoretical study, *Journal of Molecular Modeling*, 19, (2013), 1435-1444 https://doi.org/10.1007/s00894-012-1698-3

[12] I. Flaming, Molecular Orbital Theory, in: *Molecular Orbitals and Organic Chemical Reactions*, John Wiley & Sons, Ltd., 2010, https://doi.org/10.1002/9780470689493.ch1

[13] Jascha Melomedov, Julian Robert Ochsmann, Michael Meister, Frédéric Laquai, Katja Heinze, Tuning Reductive and Oxidative Photoinduced Electron Transfer in Amide-Linked Anthraquinone–Porphyrin–Ferrocene Architectures, *European Journal of Inorganic Chemistry*, 2014, 11, (2014), 1984-2001 https://doi.org/10.1002/ejic.201400118

[14] Hua Lu, ShuShu Zhang, HanZhuang Liu, YanWei Wang, Zhen Shen, ChunGen Liu, XiaoZeng You, Experimentation and Theoretic Calculation of a BODIPY Sensor Based on Photoinduced Electron Transfer for Ions Detection, *The Journal of Physical Chemistry A*, 113, 51, (2009), 14081-14086 https://doi.org/10.1021/jp907331q

[15] Bilge Turfan, Engin U. Akkaya, Modulation of Boradiazaindacene Emission by Cation-Mediated Oxidative PET, *Organic Letters*, 4, 17, (2002), 2857-2859 https://doi.org/10.1021/ol026245t

[16] Selin Manoj Kumar, Dhanapal Jothi, Sathishkumar Munusamy, Saravanan Enbanathan, Sathiyanarayanan Kulathu Iyer, Imidazole-derived new colorimetric/fluorometric chemosensor for the sensitive recognition of CN^- ions: Real-time application in food samples and fluorescence bio-imaging, *Journal of Photochemistry and Photobiology A: Chemistry*, 434, (2023), 114269 https://doi.org/10.1016/j.jphotochem.2022.114269

[17] Venkatesan Muthukumar, Sathiyanarayanan Kulathu Iyer, A simple and optically responsive chemosensor for the detection of Al^{3+} and Cr^{3+}: In live cells and real sample analysis, *Inorganic Chemistry Communications*, 122, (2020), 108289 https://doi.org/10.1016/j.inoche.2020.108289

[18] Deblina Sarkar, Ajoy Kumar Pramanik, Tapan Kumar Mondal, Coumarin based fluorescent 'turn-on' chemosensor for Zn^{2+}: An experimental and theoretical study, *Journal of Luminescence*, 146, (2014), 480-485 https://doi.org/10.1016/j.jlumin.2013.09.080

[19] M. J. Frisch, G. W. Trucks, H. B. Schlegel, G. E. Scuseria, M. A. Robb, J. R. Cheeseman, G. Scalmani, V. Barone, B. Mennucci, G. A. Petersson, in: Gaussian Inc, 2010,

[20] S. F. Boys, F. Bernardi, The calculation of small molecular interactions by the differences of separate total energies. Some procedures with reduced errors, *Molecular Physics*, 19, 4, (1970), 553-566 https://doi.org/10.1080/00268977000101561

[21] Frank Jensen, *Introduction to Computational Chemistry*, 2nd ed., Wiley, United States, 1999,

[22] Denis Jacquemin, Eric A. Perpète, Ilaria Ciofini, Carlo Adamo, Rosendo Valero, Yan Zhao, Donald G. Truhlar, On the Performances of the M06 Family of Density Functionals for Electronic Excitation Energies, *Journal of Chemical Theory and Computation*, 6, 7, (2010), 2071-2085 https://doi.org/10.1021/ct100119e

[23] Robert B. Macgregor Jr, Gregorio Weber, Fluorophores in Polar Media: Spectral Effects of The Langevin Distribution of Electrostatic Interactions, *Annals of the New York Academy of Sciences*, 366, 1, (1981), 140-154 https://doi.org/10.1111/j.1749-6632.1981.tb20751.x